LIMNOLOGY and OCEANOGRAPHY

ASLO

Limnol. Oceanogr. 66, 2021, 2051–2062

doi: 10.1002/lno.11744

Ecological stoichiometry of functional traits in a colonial harmful cyanobacterium

Zhipeng Duan [1,2] **Xiao Tan** [1*] **Hans W. Paerl** [3] **Dedmer B. Van de Waal** [2*]

[1]Key Laboratory of Integrated Regulation and Resource Development on Shallow Lakes, Ministry of Education, College of Environment, Hohai University, Nanjing, China

[2]Department of Aquatic Ecology, Netherlands Institute of Ecology (NIOO-KNAW), Wageningen, The Netherlands

[3]Institute of Marine Sciences, University of North Carolina at Chapel Hill, Morehead City, North Carolina

Abstract

Trait-based approaches provide a mechanistic framework crossing scales from cellular traits to community dynamics, while ecological stoichiometry applies first principles to understand how the balance of energy and elements shape ecological interactions. However, few studies have explicitly linked both frameworks. In this study, we tested the stoichiometric regulation of a number of carbon (C) based (e.g., extracellular polysaccharides and colony formation) and nitrogen (N) containing traits (i.e., chlorophyll *a*, phycocyanin, and gas vesicle content) in cyanobacteria in laboratory experiments and in the field. We exposed the cosmopolitan colony forming freshwater cyanobacterium *Microcystis* sp. in batch experiments to light, N and phosphorus (P) limitation, and enhanced CO_2 levels, and assessed the regulation of these traits. Cyanobacterial traits followed stoichiometrically predictable patterns, where N containing traits increased with cellular N content, and decreased with increasing C : N ratios. C-based traits increased with cellular C content and C : N ratios under nutrient, particularly N, limitation. The pattern of colony formation was confirmed with field data from Lake Taihu (China), showing an increase in colony size when N was limiting and N : P ratios were low. These findings demonstrate how an explicit coupling of trait-based approaches to ecological stoichiometry can support our mechanistic understanding of responses of cyanobacteria toward shifts in resource availability.

Changes in the global environment are expected to strongly affect the structure and functioning of aquatic ecosystems worldwide (Paerl and Huisman 2009; Huisman et al. 2018). Understanding and predicting the implications of shifts in resource availability are major challenges in aquatic ecology (Litchman et al. 2015), including the scaling across spatial and temporal dimensions. Functional traits of a species determine its growth, survival, and population dynamics under changing biotic and abiotic environmental conditions (McGill et al. 2006). Consequently, trait-based approaches allow scaling, from fundamental processes at the cellular level to dynamics at the population and community level (Edwards et al. 2013; Weithoff and Beisner 2019). Functional traits reflect a combination of distinct metabolic processes with specific underlying chemical and structural properties (Peñuelas et al. 2019), and may be inherently linked to the elemental composition of an organism (Meunier et al. 2017). Ecological stoichiometry addresses the balance of elements in organisms and their interaction with the environment (Sterner and Elser 2002). Specifically, ecological stoichiometry allows the coupling of distinct elemental ratios to biochemistry, and thereby provides a mechanistic basis for understanding the regulation of traits (Meunier et al. 2017). The linkage of elemental composition to functional traits, and functional traits to population and community interactions allows scaling from impacts of changing resource availabilities on cellular processes to altered community dynamics (Fig. 1).

Phytoplankton form the base of many aquatic food webs, and account for approximately half of the global primary production (Falkowski et al. 1998). Some species can produce toxic metabolites and under favorable conditions may proliferate to form harmful algal blooms (Smith 2003; Wells

*Correspondence: tanxiao@hhu.edu.cn (X.T.); d.vandewaal@nioo.knaw.nl (D.B.V.d.W.)

Additional Supporting Information may be found in the online version of this article.

Author Contribution Statement: Z.D. and D.B.V.d.W. designed the experiment; Z.D. acquired the data; Z.D., X.T., and D.B.V.d.W. performed the data analysis; and all authors contributed to data interpretation; Z.D. and D.B.V.d.W. wrote a first version of the manuscript; H.W.P. performed careful editing of versions of the manuscript; and all authors contributed to the final revision of the manuscript.

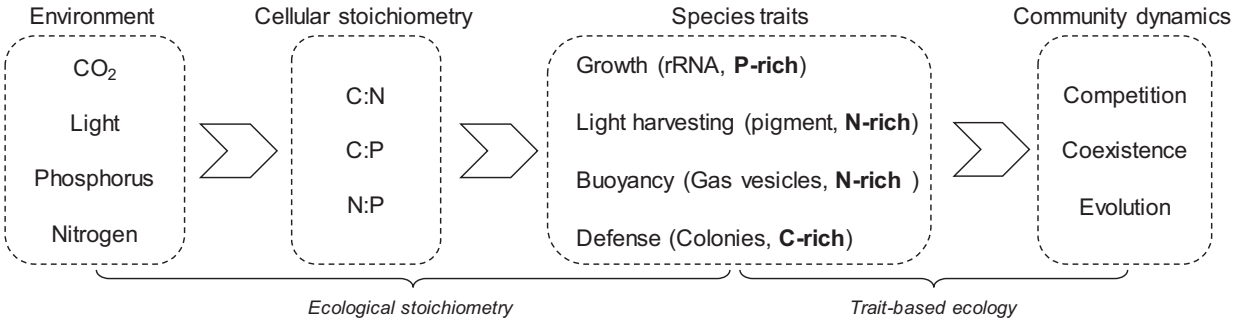

Fig. 1. Schematic overview on the integration of ecological stoichiometry and trait-based ecology for studying a colonial bloom-forming cyanobacterium.

et al. 2015). In freshwater ecosystems, harmful blooms by cyanobacteria are promoted by eutrophication (Paerl 1988; Huisman et al. 2018), and climate change is expected to exacerbate these blooms (Paerl and Huisman 2009). Although cyanobacteria generally grow relatively slow compared to their eukaryotic algal competitors (Reynolds 2006; Lürling et al. 2013), they possess a number of defensive and competitive traits facilitating their proliferation (Huisman et al. 2018). Specifically, colony formation or aggregation, a key functional trait of some bloom-forming cyanobacteria (Walsby et al. 1997), often limits the suitability of cyanobacteria as food for filter feeding zooplankton (Gerphagnon et al. 2015). Gas vesicles, another key functional trait of bloom-forming cyanobacteria, provide them with buoyancy (Walsby 1994), resulting a "shading effect" on other phytoplankton (Reynolds 2006). Both colony formation and buoyancy promote the motility of cyanobacteria, that is, through vertical migration and horizontal transport of buoyant populations (George and Edwards 1976), particular in stratified waters enhanced by seasonal and climatic warming (Paerl and Huisman 2009). Light-harvesting pigments of cyanobacteria, mainly phycocyanin, can effectively absorb photons in the orange-red part of the visible spectrum (620–630 nm), which dominates the underwater light spectra in eutrophic waters, and thus facilitate their competition for light in these regions (Stomp et al. 2007).

Traits rely on specific biomolecules or biochemical processes and may thereby exhibit distinct elemental composition (Geider and La Roche 2002; Meunier et al. 2017). For example, buoyancy is provided by gas vesicles that are relatively N-rich ($\sim$ 16% N content), as they are composed entirely of proteins (Walsby 1994). In comparison, photosynthesis obtains energy through light-harvesting pigments, which are also relatively rich in N (9.6% N content in phycocyanin and 6.3% N content in chlorophyll *a* [Chl *a*]). Colony formation depends on the synthesis and secretion of extracellular polysaccharides (EPS) that are C-rich matrices ($\sim$ 40% C; Pereira et al. 2009) in which cells cluster together from cell division and/or aggregation of existing cells (Duan et al. 2018). Thus, functional traits in colony-forming cyanobacteria can possibly be linked to their cellular stoichiometry.

Here, we explicitly link ecological stoichiometry and trait-based ecology by experimentally testing how shifts in resource availabilities (N, P, and light limitation and elevated CO_2 partial pressure [pCO_2]) alter the elemental composition and a number of key traits in *Microcystis*, a cosmopolitan colony-forming harmful cyanobacterial genus responsible for blooms in freshwater lakes worldwide (Harke et al. 2016). We hypothesized decreases in N-rich traits, such as gas vesicles and light-harvesting pigments, under N limitation, while expecting these traits to increase under P limitation when N is in relative excess. For the C-based traits, including EPS and colony formation, we hypothesized that both traits would increase under both N and P limitation. We furthermore expected higher cellular C levels and enhanced EPS and colony formation with elevated pCO_2, and an increase in N content with greater light-harvesting pigment requirements under light limitation. Lastly, we tested whether the laboratory findings were consistent with field observations, specifically testing whether colony formation was more pronounced when N and P were limiting.

Materials and methods

Culture methods and experimental design

Experiments were conducted using a colonial *Microcystis* sp. strain that was isolated from Meiliang Bay of Lake Taihu (31°24′58″N, 120°12′10″E) in August 2016. This lake is the third largest freshwater lake in China and has suffered from severe *Microcystis* spp. blooms over the past decades (Xu et al. 2010). More information on the isolation processes of the *Microcystis* sp. strain can be found in Duan et al. (2018). This strain was maintained in a temperature and light controlled incubator (Snijders Labs, Tilburg, The Netherlands) with modified WC-medium (Guillard and Lorenzen 1972) containing 6000 μmol L^{-1} NO_3^- and 300 μmol L^{-1} PO_4^{3-} (Supporting Information Table S1) grown at 24°C and a mean light intensity of 33 μmol photons m^{-2} s^{-1} with a 13 : 11 h light : dark cycle that is comparable to the light cycle of Lake Taihu in summer.

For the experiment, we applied four treatments through adjusting resource availabilities, including N limitation (–N, 100 μmol L^{-1} N), P limitation (–P, 3.5 μmol L^{-1} P), light limitation

(–Light, a low light intensity at 5 μmol photons m^{-2} s^{-1} that was obtained by placing neutral density filters between the light source and the culturing flasks), and CO_2 addition (+CO_2), and a nutrient and light replete control (for detailed experimental conditions and the experimental setup, see Supporting Information Table S1 and Fig. S1). Compressed air was provided to the headspace (Supporting Information Fig. S1), along with elevated pCO_2 mixed for the +CO_2 treatment to a level of 1000 μatm which resembles a high pCO_2 scenario for 2100 (IPCC 2014; RCP8.5). Washing bottles were added to humidify the air before it flowed into the culture flasks (Supporting Information Fig. S1). Sterile deionized water was added to the culture flasks to compensate for evaporation losses. The experiment was performed in water baths at 27°C, representing the average water temperature of Lake Taihu in summer (Xu et al. 2010). Prior to the experiment, in order to reduce the potential effect of historic culturing conditions, cultures were acclimatized respectively to the experimental conditions of each treatment for about four generations by two consecutive transfers (6–10 d). After acclimation, cultures were grown in 500 mL Erlenmeyer flasks containing 400 mL of growth medium with four replicates of each treatment. Flasks were gently mixed and randomly repositioned three times a day. The starting cell density was 1×10^5 cells mL^{-1} for each treatment. For growth assessment, all cultures were sampled daily, except the light-limited treatment that was sampled every 2 d because of the slow growth rate. These samples were used to determine cell density and biovolume using a Multisizer 3 coulter counter (Beckman Counter Life Science, Indianapolis, U.S.A.) with an aperture size of 100 μm. In the same samples, pH was measured using a calibrated inoLab® pH-7310 meter (Xylem Analytics Germany Sales GmbH & Co. KG, WTW, Weilheim, Germany). Prior to cell counting, 0.1 mL of culture suspension was diluted 100 times with deionized water and incubated for 1 h at 4°C to disperse colonies into single cells (Duan et al. 2018). An example of colony dispersion in deionized water is provided in the Supporting Information Fig. S2. Cultures were harvested for the assessment of functional traits at early stationary growth. Growth curves of all treatments and changes in pH of the culture suspensions can be found in the Supporting Information Fig. S3b.

Analyses of functional traits

We focused on five key functional traits: (1) cell size (CS) was measured as biovolume per cell using the coulter counter. (2) Specific growth rate (μ) was calculated for each replicate by fitting an exponential function through the cell count data acquired during the exponential growth phase: $N_t = N_o \exp^{\mu t}$, where N_o is the cell density at the beginning of exponential growth phase, and N_t refers to the cell density at time t. (3) Colony formation (CF) was expressed as percentage of colonial cells. To assess the number of cells in the colonies (i.e., CF), we transferred the culture material over a 15 μm sieve and thereby collected the filtrate (including single cells and very small colonies < 15 μm). We subsequently dispersed this fraction into single cells using deionized water, and analyzed the population density in this fraction (C_s) with the Coulter counter as mentioned above. Additional culture material was taken and the population density was analyzed as the total fraction (C_t) after the colonies were dispersed using deionized water. We then took the difference between C_t and C_s relative to C_t as the fraction of cells in colonies, and used this as an indicator for colony formation. Accordingly, CF was calculated to CF = $(C_t - C_s)/C_t \times 100\%$. We note that this fraction does not include very small colonies < 15 μm that only contain a few cells. The colony size of the *Microcystis* strain used here ranged from ten to hundreds of micrometers (Supporting Information Fig. S4). (4) Light-harvesting pigments, phycocyanin (PC) and Chl *a*, were extracted and measured as light-harvesting traits. Phycocyanin was extracted using the freeze-thaw method as described by Horváth et al. (2013), and then measured spectrophotometrically using a Synergy™ HT Multi-Mode microplate reader (BioTek, Winooski, Vermont, U.S.A.). The measured values were calibrated to a standard C-phycocyanin that was extracted from *Spirulina* sp. (Sigma-Aldrich, Darmstadt, Germany; R^2 = 0.99). Chl *a* was extracted using 80% ethanol at 80°C for 10 min, and then measured using an Ultimate 3000 high-performance liquid chromatograph (ThermoFisher, Waltham, Massachusetts, U.S.A.). (5) The relative amount of gas vesicles (GV) was estimated as percentage of cells with gas vesicles using a BD Influx™ flow cytometer (BD Biosciences, San Jose, California, U.S.A.) according to a method modified from Lee et al. (2000). In short, the sample of each replicate was split evenly into two fractions. Gas vesicles in cells of one subgroup were collapsed sonically (Lee et al. 2000; Rodriguez-Molares et al. 2014). Both fractions were analyzed using flow cytometry and the location of cells in the plots of side scatter (SSC) vs. forward scatter (FSC) was recorded. This allowed gating the sonicated cell cluster without gas vesicles, as this cluster was present at low SSC and relative higher FSC in the collapsed samples but showed a marked increase in SSC and a decrease in FSC in the uncollapsed samples (Supporting Information Fig. S5). In the original samples (the uncollapsed fraction), cells with higher SSC and located outside the boundaries of the gate were recorded as cells with gas vesicles (C_{gv}). Based on these fractions, GV was estimated according to GV=C_{gv}/$C_{total} \times 100\%$, where C_{total} is the total count of cells (for details on the GV estimation, see Supporting Information Fig. S5). Note that this method is not a direct measurement of the absolute volume of gas vesicles as described by Walsby (1994). However, the signal of SSC is strongly correlated to the volume of gas vesicles (Supporting Information Fig. S6), although there was somewhat of an underestimation of the mean relative GV under light limitation. Therefore, it should be considered as an estimation of the gas vesicle content (Lee et al. 2000; Rodriguez-Molares et al. 2014).

Cellular C, N, and P contents

Cellular C, N, and P were determined at early stationary growth by collecting 5–25 mL of cultures on prewashed (100 mL distilled water) GF/F filters (Whatman, Maidstone, UK). Filters were dried overnight at 60°C and stored in a

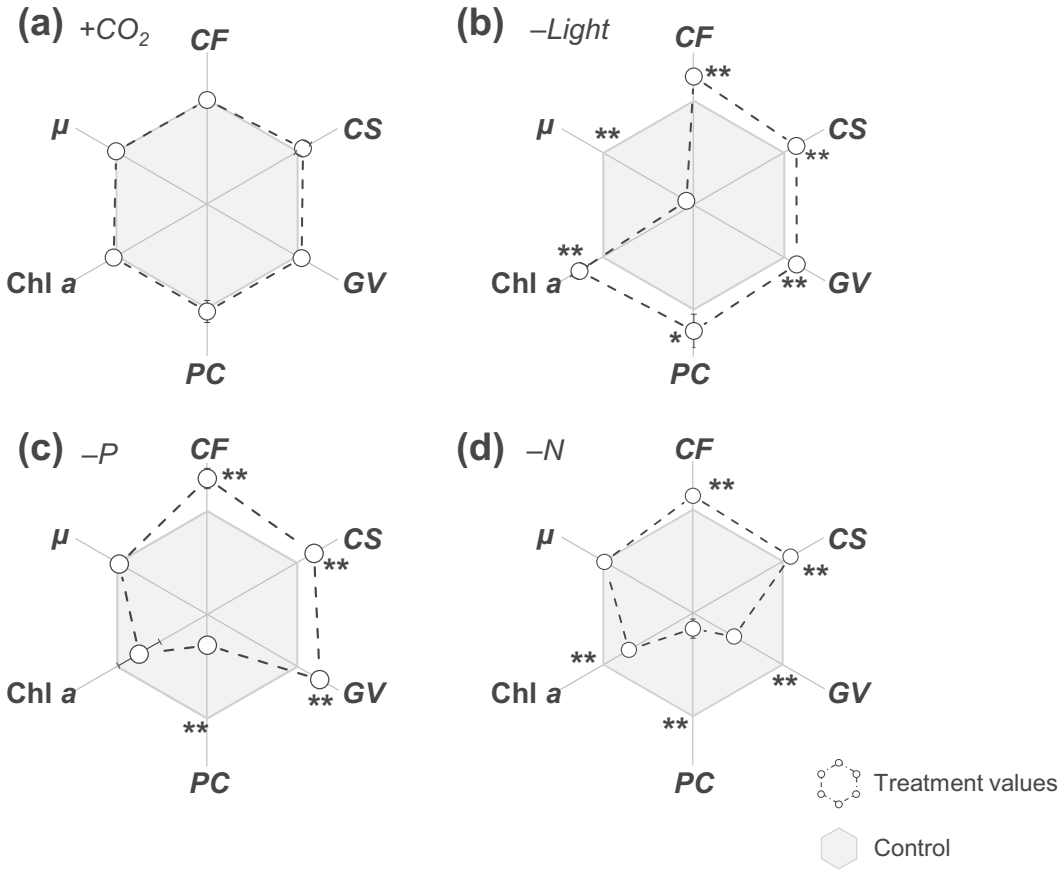

Fig. 2. Functional traits of *Microcystis* responding to different environmental variables, with (**a**) CO_2 addition ($+CO_2$), (**b**) light-limitation (–Light), (**c**) P-limitation (–P), and (**d**) N-limitation (–N). Each point shows a measured functional trait, including colony formation (CF), cell size (CS), gas vesicles (GV), light-harvesting traits phycocyanin (PC) and Chl *a*, and specific growth rate (μ). The dashed lines represent the log response ratio of the traits in the treatments compared to those of the control (the gray background). Error bars denote the standard deviation (SD) ($n = 4$). Significance levels are indicated by the asterisks * ($p < 0.05$) and ** ($p < 0.01$).

desiccator in darkness. For cellular C and N analyses, a subsample (16%) of each filter was taken by a presterilized hole puncher, folded into a tin cup and analyzed on a FLASH 2000 organic elemental analyzer (Brechbueler Incorporated, Interscience B.V., Breda, The Netherlands). Cellular P was analyzed by combusting the remainder of the filter (84%) for 30 min at 550°C in Pyrex glass tubes, followed by a digestion step with 5 mL persulfate (2.5%) for 30 min at 120°C. This digested solution was determined for PO_4^{3-} on a QuAAtro AutoAnalyzer (SEAL Analytical, Southampton, UK).

Extracellular organic carbon allocation

For estimation of carbon allocation of the cultures under different treatments, extracellular organic carbon of the cultures including bound EPS and dissolved organic matter (DOM) in the filtered samples was analyzed. A thermal method that has been developed and evaluated on extraction efficiency and cell integrity in our previous work was applied to extract the bound EPS (Duan et al. 2020). Specifically, 50 mL of the cultures was pipetted into a tube and then centrifuged at 5000 rpm for 10 min. The pellets were resuspended into the original volumes using a borate buffer (0.49 mmol L^{-1} H_3BO_3, 0.2 mmol L^{-1} $Na_2B_4O_7$, and 85 mmol L^{-1} NaCl, pH = 8.4). The suspensions were heated at 65°C for 30 min, and then rapidly cooled to room temperature in an ice bath. The cooled suspension was filtered (GF/F, Whatman, Maidstone, UK), and the filtrate containing the bound EPS was collected and stored at 4°C until analysis. Carbon allocation in the DOM of the media was determined as well. Cultures were filtered (GF/F, Whatman), and the filtrate containing the DOM was collected and stored at 4°C prior to further analysis. Dissolved organic carbon in these filtrates was analyzed within 7 d using an E200 TOC-LCPH total organic carbon analyzer (Shimadzu Benelux B.V., Wemmel, Belgium).

Field data collection and data analysis

To test how nutrient availability affects colony formation of *Microcystis* spp. in the field, we collected and reanalyzed data that were extracted from published studies (Zhu et al. 2016, 2018*a*,*b*) using, Engauge Digitizer software version 4.1 (Mitchell et al. 1991). This field data set includes monthly averages of total dissolved nitrogen (TDN), total dissolved phosphorus (TDP), and phytoplankton biomass (measured

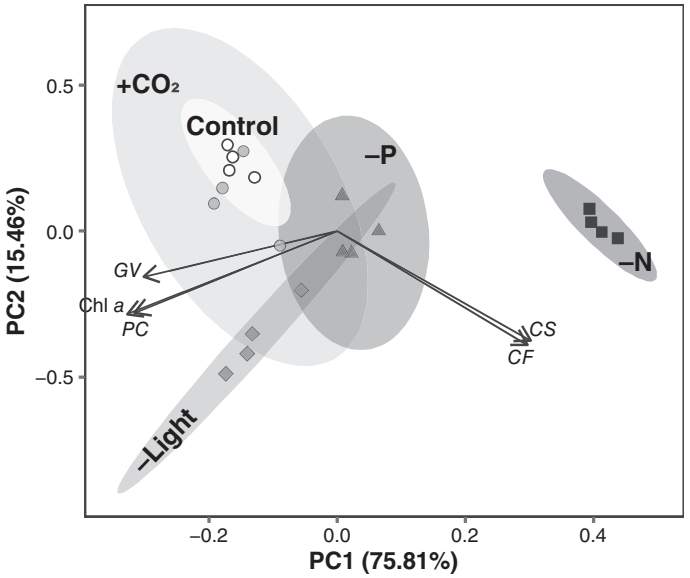

Fig. 3. PCA plot of the total variation in the functional traits responding to different treatments. Each ellipse groups a biological replicate according to the treatments with control, CO_2 addition ($+CO_2$), N-limitation (–N), P-limitation (–P), or light-limitation (–Light). The tested functional traits include colony formation (CF), cell size (CS), gas vesicles (GV), and light-harvesting pigments phycocyanin (PC) and Chl *a*.

as Chl *a* concentration) in Meiliang Bay of Lake Taihu from April 2011 to November 2013, and were originally acquired by the Taihu Laboratory for Lake Ecosystem Research (TLLER) (Zhu et al. 2018*a*). Monthly average data of total nitrogen (TN) and total phosphorus (TP) in Meiliang Bay of Lake Taihu during the same periods were extracted from a published data set (Zhu et al. 2018*b*). Based on the nutrient concentrations, we calculated the TN : TP and TDN : TDP ratios. Monthly average data of colony size in *Microcystis* spp. were measured in Meiliang Bay of Lake Taihu during the same sampling period (Zhu et al. 2016). Specifically, the colony size was determined by measuring the diameter of colonies on images from light microscopy (for details, see Zhu et al. 2016). These data can be found in the Supporting Information Table S2.

All statistics were conducted in R version 3.5.2 (R Core Team 2018). We assessed the effect of the treatments on the tested functional traits (i.e., CS, μ, CF, PC, Chl *a*, and GV) through calculating a log response ratio as $\ln(B_{i,t}/B_{i,c})$ where $B_{i,t}$ is the value of functional trait i under the treatment t (i.e., $+CO_2$, –Light, –P, or –N) and $B_{i,c}$ is the value of functional trait i in the control. Significant differences in the expression of the trait under a treatment compared to that of the control were analyzed using a one-way ANOVA with significant levels

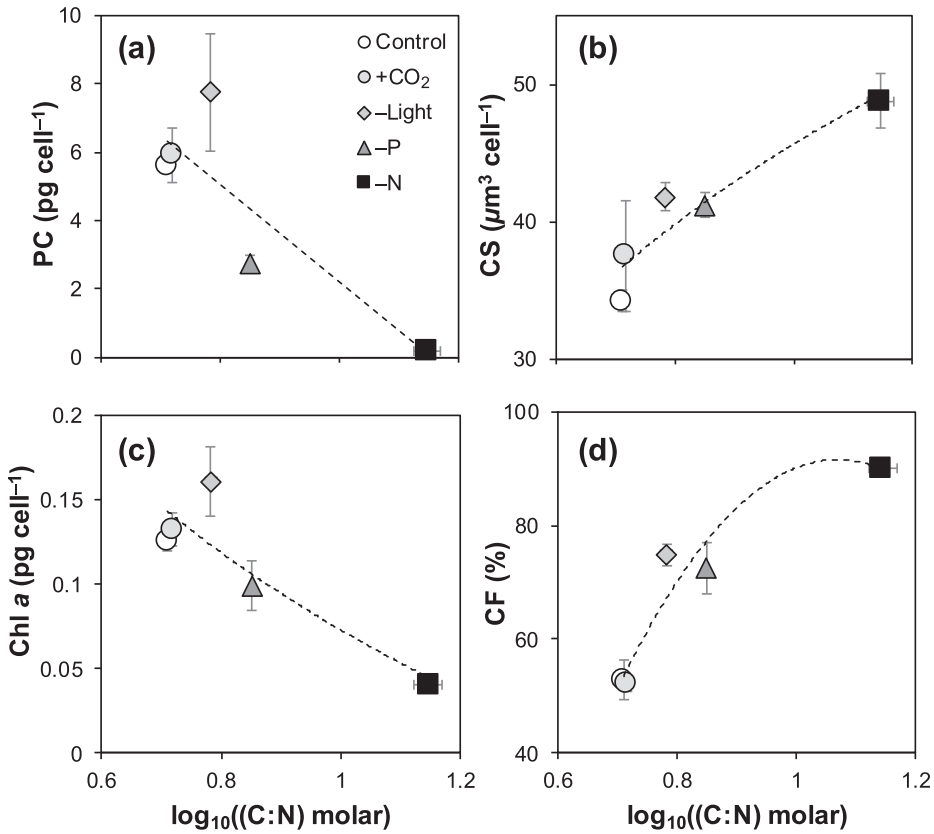

Fig. 4. Relationships between functional traits and cellular C : N ratio (log) across all the treatments. A two-order polynomial model fitted the correlations in (**c**) and (**d**), logarithmic regression in (**b**) and linear regression in (**a**). The tested functional traits include colony formation (CF), cell size (CS), gas vesicles (GV), and light-harvesting pigments phycocyanin (PC) and Chl *a*. Error bars denote the SD (n = 4).

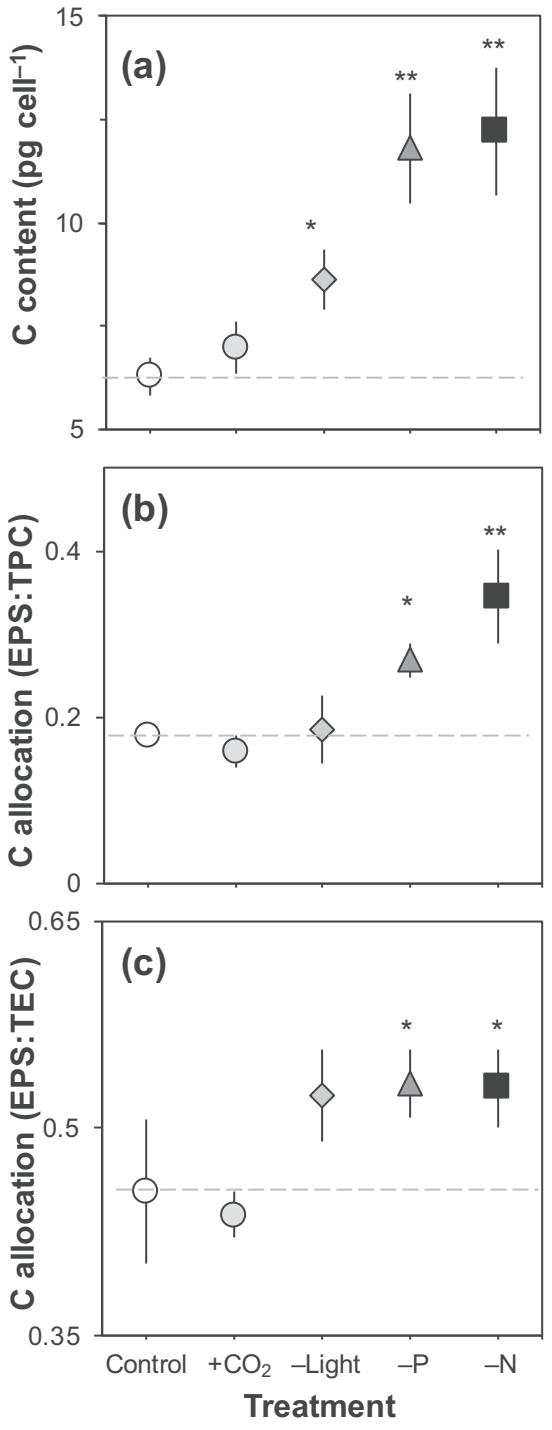

Fig. 5. Accumulation and allocation of organic carbon in the different treatments with (**a**) the C content per cell, (**b**) the allocation to extracellular polymeric substances (EPS) relative to the total particulate organic carbon (TPC), and (**c**) the allocation to EPS relative to the total extracellular organic carbon (TEC). The treatments include a control, CO_2 addition ($+CO_2$), N-limitation (–N), P-limitation (–P), and light-limitation (–Light). Error bars denote the SD ($n = 4$). Significance levels are indicated by the asterisks * ($p < 0.05$) and ** ($p < 0.01$).

of $p < 0.05$ (*) and $p < 0.01$ (**). Principal component analysis (PCA) was performed using the "prcomp" function in the "stats" package of R to explore the potential correlation between traits from the laboratory experimental data or between nutrient and colony size of *Microcystis* spp. from the field data. Linear regression was conducted to assess the relationships among traits, and four linear and nonlinear regression models were used to assess the relationships between traits and the cellular C and N contents, and C : N ratios across all the treatments using our experimental data. The models with the minimum Akaike information criterion values chosen (Supporting Information Tables S3, S4). The relationships between colony size and field environmental variables were evaluated using linear regression. Partial redundancy analysis was conducted to isolate the contributions of different sets of constraints (Legendre et al. 2011): nutrient concentration (TN, TP, TDN, and TDP), nutrient ratios (TN : TP and TDN : TDP), phytoplankton biomass (Chl *a* concentration), and their covariables, to colony size in the field using the "vegan" package in R (Oksanen et al. 2015). The significance of those sets of constraints was tested by a permutation test, and displayed in a Venn diagram.

Results

Functional traits of the *Microcystis* sp. tested in our study differed in response to environmental variables, especially under light- and nutrient-limited conditions, but no significant changes were observed in response to CO_2 addition (Fig. 2a). Specifically, cell size (CS), colony formation (CF), and estimated gas vesicle content (GV) significantly increased in response to both light and P limitation (Fig. 2b,c). Under N limitation, colony formation increased while gas vesicles and light-harvesting pigments (PC and Chl *a*) were inhibited (Fig. 2d). The cultures experiencing N limitation were clearly separated from the cultures of other treatments under the first PCA axis (PC1) that explained 75.8% of the total variation. PC1 was positively associated with colony formation and cell size, but negatively with GV, PC, and Chl *a* (Fig. 3). We also observed positive correlations between some functional traits (Fig. 3), including colony formation and cell size (linear regression, $R^2 = 0.81$, $p < 0.0001$, $n = 20$), and both light-harvesting pigments (linear regression, $R^2 = 0.95$, $p < 0.0001$, $n = 20$).

For several traits, we observed clear and predictable relationships with the cellular stoichiometry (Fig. 4). The estimated gas vesicle content increased with cellular N content (nonlinear quadratic regression, goodness of fit = 0.91, $n = 20$; Supporting Information Table S4 and Fig. S7a), while cell size (linear regression, $R^2 = 0.64$, $p < 0.0001$, $n = 20$) and colony formation (linear regression, $R^2 = 0.73$, $p < 0.0001$, $n = 20$) were positively correlated with cellular C content (Supporting Information Table S4 and Fig. S7e,f). Moreover, the light-harvesting pigments PC (linear regression, $R^2 = 0.69$, $p < 0.0001$, $n = 20$) and Chl *a* (linear regression, $R^2 = 0.73$, $p < 0.0001$, $n = 20$) decreased with cellular C : N ratios (Fig. 4a,c), while both colony formation (nonlinear

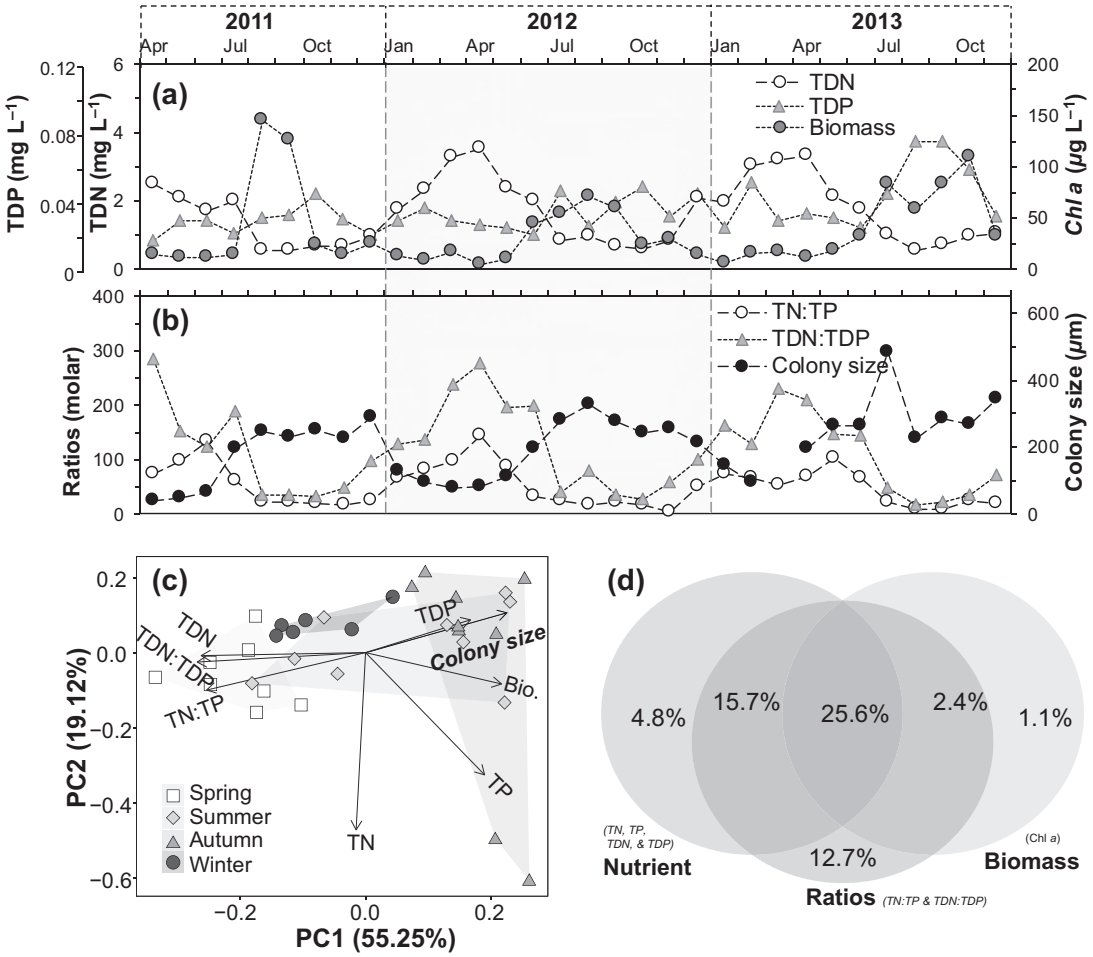

Fig. 6. Overview of relationships between colony size, nutrient availabilities, and phytoplankton biomass in Lake Taihu (Meiliang Bay, China), from April 2011 to November 2013. (**a**) Changes in TDN, TDP, and biomass (Bio.) in this period. (**b**) Changes in TDN : TDP, TN : TP, and colony size in this period. (**c**) PCA with relationships between nutrient concentrations (TN, TP, TDN, TDP) and ratios (TN : TP, TDN : TDP), Chl *a* concentration, and colony size. (**d**) Venn diagram depicting the relative contributions of nutrient concentrations (TN, TP, TDN, TDP), ratios (TN : TP, TDN : TDP), and biomass (Chl *a*) to colony size. Panel (**a**) was redrawn from Zhu et al. (2018*a*) with permission from the Nanjing Institute of Geography and Limnology, Chinese Academy of Sciences (NIGLAS). Panels (**b**)–(**d**) were reanalyzed based on the data extracted from Zhu et al. (2016), Zhu et al. (2018*a*), and Zhu et al. (2018*b*).

quadratic regression, goodness of fit = 0.94, $n = 20$) and cell size (nonlinear logarithmic regression, goodness of fit = 0.77, $p < 0.0001$, $n = 20$) increased with cellular C : N ratio (Fig. 4b,d; Supporting Information Table S4). For the estimated gas vesicle content, we observed an optimum at intermediate C : N ratios (Supporting Information Fig. S7d). Specifically, the contribution of cells with gas vesicles increased from low to intermediate C : N ratios approaching Redfield ratio (i.e., ~ 6.7), after which it decreased with a further increase in cellular C : N ratio as result of N limitation.

Both colony formation and cell size were promoted under nutrient limited conditions, especially under N limitation, and both traits showed a "V-shaped" response to the cellular N : P ratio (Supporting Information Fig. S8). Nutrient limited conditions caused a large amount of C accumulation in the cyanobacterial cells (Fig. 5a). Compared to the control, EPS increased by 94% and 50% under N and P limitation, respectively (Fig. 5b). With regard to secreted organic C, ~ 53% was associated with cells as bound EPS under light and nutrient limited conditions, while approximately 55–57% was dissolved in the media of the control and CO_2 addition treatments (Fig. 5c).

The field data showed clear seasonal variation in nutrients and phytoplankton biomass (as Chl *a* concentration) in Meiliang Bay, where higher TDN, TDN : TDP, and TN : TP were observed in winter and spring, while higher TP, TDP, phytoplankton biomass, and large-size colonies occurred in summer and autumn (Fig. 6a,b). Based on the PCA (Fig. 6c), colony size in *Microcystis* spp. was negatively correlated with TDN (linear regression, $R^2 = 0.44$, $p < 0.001$, $n = 31$), TDN : TDP (linear regression, $R^2 = 0.45$, $p < 0.001$, $n = 31$), and TN : TP (linear regression, $R^2 = 0.53$, $p < 0.001$, $n = 31$), but positively associated with phytoplankton biomass (linear regression, $R^2 = 0.29$, $p < 0.005$, $n = 31$). No significant relationships were observed between colony size and TN (linear regression, $R^2 = 0.04$, $p = 0.281$, $n = 31$),

TDP (R^2 = 0.09, p = 0.098, n = 31), or TP (R^2 = 0.11, p = 0.076, n = 31). As shown in the Venn diagram (Fig. 6d), nutrient concentrations (TN, TP, TDN, and TDP concentrations), nutrient ratios (TN : TP and TDN : TDP), phytoplankton biomass, and the covariables explained more than 62% of the total variation of colony size in the field data. Although biomass and its covariables with nutrient concentrations and nutrient ratios together explained 29% of the total variation in colony size, biomass alone did not significantly contribute to the variation (1%; p = 0.38, permutation = 999). More than 33% of the variation was explained by the combination of nutrient and the ratios (p = 0.007, permutation = 999), while nutrient ratios alone (13%; p = 0.04, permutation = 999) explained much more of the variation than nutrient concentrations alone (5%; p = 0.55, permutation = 999).

Discussion

Our results demonstrated that the cellular stoichiometry and functional traits of *Microcystis* varied substantially in response to changes in resource availability, except for the CO_2 addition treatment (Figs. 2, 4; Supporting Information Fig. S7). For example, *Microcystis* cells accumulated a large amount of cellular C under nutrient (N and P) limited conditions, upon which cell size increased (Fig. 5a). Excess C that cannot be shunted to growth was presumably stored (see also Wagner et al. 2017), and, after maximum storage capacity was reached, excreted as EPS, thereby promoting colony formation (Figs. 2, 5). This is in line with earlier observations showing that N- and P-limited conditions enhanced EPS production in various species of phytoplankton (Otero and Vincenzini 2003; Urbani et al. 2005). Both colony formation and cell size strongly relied on the relative excess of cellular C (Supporting Information Fig. S7c,f), and increased with cellular C : N ratio (Fig. 4b,d). Other C-based traits in phytoplankton have been reported to follow stoichiometrically predictable patterns as well. For instance, C-rich toxins seem to generally increase with cellular C content under both N and P limitation (Van de Waal et al. 2014). Similarly, a range of C-rich primary metabolites, such as carbohydrates, fatty acids, and lipids, were also shown to increase under both N and P limitation (Gao et al. 2018).

We did not observe significant effects of the applied N and P limiting conditions on growth rate (Fig. 2c,d), presumably because the applied nutrient concentrations allowed maximum growth prior to reaching the nutrient depleted stationary phase (Supporting Information Fig. S3). We note that growth rate may correlate to cellular P contents, as it requires P-rich ribosomal RNA (Fig. 1; Sterner and Elser 2002; Elser et al. 2003; but see Flynn et al. 2010). Our current data, however, do not allow testing this growth rate hypothesis in *Microcystis* sp., for which a broader range in growth rates is required, together with data on ribosomal RNA contents.

The observed relationships between nutrient limitation and C allocation may result from stoichiometrically imbalanced conditions. Although N limitation reduces photosynthesis, N-depleted cyanobacterial cells (e.g., *Synechococcus*) are forced to allocate more energy going into carbohydrate synthesis (Qian et al. 2017). Moreover, it has been shown that in phytoplankton less energy is required for the synthesis of carbohydrates compared to that of proteins (Kroon and Thoms 2006). Both can lead to a significant increase in the proportion of carbohydrates to proteins in cells under N-limited conditions (Qian et al. 2017). Consequently, an increase in intracellular carbohydrates promotes the secretion of EPS (Myklestad 1995), which facilitates colony formation (Duan et al. 2018). In addition, phycocyanin has been shown to more rapidly decrease than Chl *a* when cells are N starved because phycocyanin may serve as an N reserve in cyanobacteria (Allen 1984). This was confirmed by the relatively low PC : Chl *a* ratio in the N-limited treatment (Supporting Information Fig. S9). Therefore, despite a reduction in phycocyanin contents, cells can still capture light with the remaining Chl *a* and continue C fixation (Lemasson et al. 1973), leading to C accumulation and, subsequently, enhanced colony formation.

The relationship between the limitation by N and colony formation was also observed in natural *Microcystis* spp. blooms in Meiliang Bay of Lake Taihu. As the blooms reached their peak biomass and persisted through summer into fall, N and P colimitation or exclusive N limitation tended to become more common (Xu et al. 2010). *Microcystis* colony size was enhanced during this period when N concentrations decreased (Fig. 6a), presumably as result of high N requirements for bloom formation and high rates of denitrification (Scott et al. 2019), while TDP levels remained constant or slightly increased (Fig. 6a). Consequently, colony size was generally larger when TN : TP and TDN : TDP ratios were low (Fig. 6b), indicating N limitation. We suggest that pronounced colony formation is favored by nutrient limitation, particularly under N limitation, and most of the variation in colony size was explained by nutrient stoichiometry (TN : TP and TDN : TDP ratios) rather than nutrient concentrations (TN, TP, TDN, and TDP) or biomass (Chl *a* concentration; Fig. 6d). In turn, colony formation probably benefits 'nutrient, O_2, and CO_2 exchange within the "phycosphere" by associated bacteria, thus minimizing nutrient (especially P) limitation (Paerl and Millie 1996; Cook et al. 2019). Colony formation may also benefit the buildup of *Microcystis* biomass because of the high resistance of colonies to grazing pressure from zooplankton (Gerphagnon et al. 2015), and an increased floating velocity of large colonies allowing more effective light capture in the upper water column even under wind-wave mixing (Zhao et al. 2017), which is line with the positive correlation between colony size and biomass (Fig. 6a,b). We note, however, that the opportunity for aggregation of colonial *Microcystis* may increase when there are more cells (Duan et al. 2018), and thus, alternatively, colony formation may also be promoted by high biomass.

Colony formation and cell size of *Microcystis* showed a "V-shaped" pattern in relation to the cellular N : P ratio, with the minimum value approximating the "Redfield" ratio (i.e., $\log_{10}$[N : P] = 1.2; Supporting Information Fig. S8). This suggests that *Microcystis* allocated minimum investment to the

C-based traits under N : P balanced conditions. This is in line with earlier reported relationships between C-rich traits and nutrient limitation in phytoplankton. For example, the cellular contents of C-rich metabolites including C-rich toxins (e.g., okadaic acid), lipids, and carbohydrates in phytoplankton seem to follow a general "V-shaped" response to N : P ratios (Granéli et al. 2012; Van de Waal et al. 2014; Gao et al. 2018), with lowest cellular contents under balanced conditions, and increases under both N and P limitation.

As hypothesized, the estimated amounts of N-rich gas vesicles decreased under N limitation (Fig. 2d) because less N is available for synthesizing the required proteins (Oliver and Ganf 2000). While this is potentially limiting buoyancy, it may also support vertical migration. With reduced gas vesicles, cells are more prone to sinking, and thereby passively migrate to nutrient-enriched deeper waters or sediments (Walsby et al. 1997). These nutrient-rich conditions would, in turn, promote synthesis of gas vesicles, thus enhancing buoyancy and migration of cells to the radiant-rich surface. Diel vertical migration in *Microcystis* has been associated with carbohydrate ballast (Kromkamp and Mur 1984), which can be rapidly regulated within hours (Walsby 1994). The synthesis and reformation of collapsed gas vesicles, however, was shown to be in the order of days (Walsby 1994), and it is thus unlikely to contribute to diel vertical migration of *Microcystis*. Yet, our findings do show that the responses of gas vesicle synthesis to changes in N availability at least would support the direction of vertical migration.

The Phycocyanin and Chl *a* increased substantially under light limitation (Fig. 2b), but decreased under N limitation (Fig. 2d). With reduced light, higher contents of light-harvesting pigments will allow maintenance of photosynthesis and C assimilation, and is in agreement with earlier observations (Langdon 1988; Laviale and Neveux 2011). Phycocyanin and Chl *a* are N-rich compounds that decreased with cellular C : N ratio (Fig. 4a,c). Under N limitation, phycocyanin and Chl *a* are depleted for cell division (Oliver and Ganf 2000) and C is accumulated in cells as described early, causing an increase in C : N ratio. Besides gas vesicles and pigments, other N-rich traits in phytoplankton have been reported following cellular elemental stoichiometry as well. For example, the synthesis of N-rich toxic secondary metabolites (e.g., microcystins) was shown to generally decrease upon N limitation and increase under P limitation, thus decreasing with cellular C : N ratio (Van de Waal et al. 2009; Gobler et al. 2016; Wagner et al. 2019; Brandenburg et al. 2020).

Our results illustrate that functional traits of *Microcystis* generally follow stoichiometrically predictable patterns, while in some cases it is the elemental content rather than the ratios that can explain a trait response. For example, the estimated content of gas vesicle increased slightly with the cellular C : N ratio followed by a sharp decrease at the high C : N ratio that caused by the N limitation (Supporting Information Fig. S7d). Shifts in cellular C : N ratios can be derived from changes in cellular C or N content, or both. Under light or P limitation, both cellular C and N contents increased, but the relative accumulation of cellular C was stronger than cellular N, leading to an increase in the C : N ratio. Therefore, while gas vesicles clearly followed the cellular N quota, this was not reflected by the C : N ratios (Supporting Information Fig. S7a, d). Moreover, synthesis of gas vesicles seems to directly depend on light (Oliver and Ganf 2000), following an inverse correlation with light intensity (Pfeifer 2012), which is in line with our data showing an increase in estimated gas vesicle content with light limitation (Fig. 2b), even though there was a potential underestimation of the gas vesicle content in the light limited treatment (Supporting Information Fig. S5b).

The light-harvesting pigments appeared to follow a unimodal function (Supporting Information Tables S3, S4) in response to cellular N content (Supporting Information Fig. S7b,c), which was mainly caused by a significant decrease in the pigments under the P-limited treatment. Under P limitation, cells possibly reallocated more cellular N to synthesize carriers for P acquisition or alkaline phosphatase for hydrolysis of organic P rather than pigment production (Kromkamp et al. 1989; Wang et al. 2018). Alternatively, cyanobacterial cells can store excess cellular N as cyanophycin, functioning as a N- and C-storage polypeptide consisting of arginine and aspartic acid (Allen 1984; Van de Waal et al. 2010), which may accumulate in cells when they are starved for P. Furthermore, light-harvesting pigments (e.g., phycocyanin) are degraded in P-limited cyanobacteria (Allen 1984) probably to prevent oxidative stress caused by high light intensity.

In contrast to what we expected, the CO_2 addition treatment did not result in a significant change in the functional traits and cellular stoichiometry of colonial *Microcystis*. This suggests that the colonial *Microcystis* was not limited by CO_2 under the control conditions with the current atmospheric pCO_2 ($\sim$ 350 μatm; Supporting Information Table S1). This might be attributed to the operation of effective carbon-concentrating mechanisms that can maintain internal CO_2 at near saturating levels under current atmospheric pCO_2 (Sandrini et al. 2014; Ji et al. 2020). Moreover, colonial *Microcystis* strains were shown to have a high affinity for the uptake of inorganic C, notably HCO_3^- (Wu and Song 2008), while microbes associated to colonies facilitate C cycling, which may help alleviate C limitation (Paerl and Millie 1996; Paerl and Pinckney 1996).

Our results confirm a clear coupling between cellular stoichiometry and a number of key functional traits. Although we tested a single species of *Microcystis*, some of the relationships may be more general and also apply to other phytoplankton species, particularly in response to nutrient availability. Our results demonstrate how stoichiometric regulation of traits, notably colony formation, may help explain responses of cyanobacteria to shifts in resource availability in the natural environment. Thus, by explicitly coupling functional traits to biological stoichiometry, we show how trait-based approaches are underpinned by first principles, which may be a step forward in understanding and predicting phytoplankton community dynamics in a highly dynamic environment.

Data availability statement

The data supporting the results are available in https://doi.org/10.34894/FOSVYR, DataverseNL, V1.

References

Allen, M. M. 1984. Cyanobacterial cell inclusions. Annu. Rev. Microbiol. **38**: 1–25. doi:10.1146/annurev.mi.38.100184.000245

Brandenburg, K. M., L. Siebers, J. Keuskamp, T. G. Jephcott, and D. B. Van de Waal. 2020. Effects of nutrient limitation on the synthesis of N-rich phytoplankton toxins: A meta-analysis. Toxins **4**: 221. doi:10.3390/toxins12040221

Cook, K. V., et al. 2019. The global *Microcystis* interactome. Limnol. Oceanogr. **65**: S194–S207. doi:10.1002/lno.11361

Duan, Z., X. Tan, K. Parajuli, S. Upadhyay, D. Zhang, X. Shu, and Q. Liu. 2018. Colony formation in two *Microcystis* morphotypes: Effects of temperature and nutrient availability. Harmful Algae **72**: 14–24. doi:10.1016/j.hal.2017.12.006

Duan, Z., X. Tan, D. Zhang, and K. Parajuli. 2020. Development of thermal treatment for the extraction of extracellular polymeric substances from *Microcystis*: Evaluating extraction efficiency and cell integrity. Algal Res. **48**: 101879. doi:10.1016/j.algal.2020.101879

Edwards, K. F., E. Litchman, and C. A. Klausmeier. 2013. Functional traits explain phytoplankton responses to environmental gradients across lakes of the United States. Ecology **94**: 1626–1635. doi:10.1890/12-1459.1

Elser, J. J., and others. 2003. Growth rate-stoichiometry couplings in diverse. Ecol. Lett. **6**: 936–943. doi:10.1046/j.1461-0248.2003.00518.x

Falkowski, P. G., R. T. Barber, and V. Smetacek. 1998. Biogeochemical controls and feedbacks on ocean primary production. Science **281**: 200–206. doi:10.1126/science.281.5374.200

Flynn, K. J., J. A. Raven, T. A. V. Rees, Z. Finkel, A. Quigg, and J. Beardall. 2010. Is the growth rate hypothesis applicable to microalgae?[1]. J. Phycol. **46**: 1–12. doi:10.1111/j.1529-8817.2009.00756.x

Gao, B., J. Liu, C. Zhang, and D. B. Van de Waal. 2018. Biological stoichiometry of oleaginous microalgal lipid synthesis: The role of N:P supply ratios and growth rate on microalgal elemental and biochemical composition. Algal Res. **32**: 353–361. doi:10.1016/j.algal.2018.04.019

Geider, R., and J. La Roche. 2002. Redfield revisited: Variability of C:N:P in marine microalgae and its biochemical basis. Eur. J. Phycol. **37**: 1–17. doi:10.1017/S0967026201003456

George, D. G., and R. W. Edwards. 1976. The effect of wind on the distribution of chlorophyll *a* and crustacean plankton in a shallow eutrophic reservoir. J. Appl. Ecol. **13**: 667–690. doi:10.2307/2402246

Gerphagnon, M., D. J. Macarthur, D. Latour, C. M. M. Gachon, F. Van Ogtrop, F. H. Gleason, and T. Sime-Ngando. 2015. Microbial players involved in the decline of filamentous and colonial cyanobacterial blooms with a focus on fungal parasitism. Environ. Microbiol. **17**: 2573–2587. doi:10.1111/1462-2920.12860

Gobler, C. J., J. M. Burkholder, T. W. Davis, M. J. Harke, T. Johengen, C. A. Stow, and D. B. Van de Waal. 2016. The dual role of nitrogen supply in controlling the growth and toxicity of cyanobacterial blooms. Harmful Algae **54**: 87–97. doi:10.1016/j.hal.2016.01.010

Granéli, E., B. Edvardsen, D. L. Roelke, and J. A. Hagström. 2012. The ecophysiology and bloom dynamics of *Prymnesium* spp. Harmful Algae **14**: 260–270. doi:10.1016/j.hal.2011.10.024

Guillard, R. R., and C. J. Lorenzen. 1972. Yellow-green algae with chlorophyllide. J. Phycol. **8**: 10–14. doi:10.1111/j.1529-8817.1972.tb03995.x

Harke, M. J., M. M. Steffen, C. J. Gobler, T. G. Otten, S. W. Wilhelm, S. A. Wood, and H. W. Paerl. 2016. A review of the global ecology, genomics, and biogeography of the toxic cyanobacterium, *Microcystis* spp. Harmful Algae **54**: 4–20. doi:10.1016/j.hal.2015.12.007

Horváth, H., A. W. Kovács, C. Riddick, and M. Présing. 2013. Extraction methods for phycocyanin determination in freshwater filamentous cyanobacteria and their application in a shallow lake. Eur. J. Phycol. **48**: 278–286. doi:10.1080/09670262.2013.821525

Huisman, J., G. A. Codd, H. W. Paerl, B. W. Ibelings, J. M. Verspagen, and P. M. Visser. 2018. Cyanobacterial blooms. Nat. Rev. Microbiol. **16**: 471–483. doi:10.1038/s41579-018-0040-1

IPCC. 2014. Climate Change 2014: Synthesis report, p. 74. Contribution of working groups I, II and III to the fifth assessment report of the Intergovernmental Panel on Climate Change. IPCC.

Ji, X., J. M. H. Verspagen, D. B. Van de Waal, B. Rost, and J. Huisman. 2020. Physiological acclimation to elevated CO_2 will intensify cyanobacterial blooms in lakes. Sci. Adv. **6**: eaax2926. doi:10.1126/sciadv.aax2926

Kromkamp, J., A. van den Heuvel, and L. R. Mur. 1989. Phosphorus uptake and photosynthesis by phosphate-limited cultures of the cyanobacterium *Microcystis aeruginosa*. Br. Phycol. J. **24**: 347–355. doi:10.1080/00071618900650361

Kromkamp, J. C., and L. R. Mur. 1984. Buoyant density changes in the cyanobacterium *Microcystis aeruginosa* due to changes in the cellular carbohydrate content. FEMS Microbiol. Lett. **25**: 105–109. doi:10.1111/j.1574-6968.1984.tb01384.x

Kroon, B. M. A., and S. Thoms. 2006. From electron to biomass: A mechanistic model to describe phytoplankton photosynthesis and steady-state growth rates. J. Phycol. **42**: 593–609. doi:10.1111/j.1529-8817.2006.00221.x

Langdon, C. 1988. On the causes of interspecific differences in the growth-irradiance relationship for phytoplankton. II. A general review. J. Plankton Res. **10**: 1291–1312. doi:10.1093/plankt/10.6.1291

Laviale, M., and J. Neveux. 2011. Relationships between pigment ratios and growth irradiance in 11 marine phytoplankton species. Mar. Ecol. Prog. Ser. **425**: 63–77. doi:10.3354/meps09013

Lee, T. J., K. Nakano, and M. Matsumura. 2000. A new method for the rapid evaluation of gas vacuoles regeneration and viability of cyanobacteria by flow cytometry. Biotechnol. Lett. **22**: 1833–1838. doi:10.1023/A:1005653124437

Legendre, P., J. Oksanen, and C. J. ter Braak. 2011. Testing the significance of canonical axes in redundancy analysis. Methods Ecol. Evol. **2**: 269–277. doi:10.1111/j.2041-210X.2010.00078.x

Lemasson, C., N. T. De Marsac, and G. Cohen-Bazire. 1973. Role of allophycocyanin as a light-harvesting pigment in cyanobacteria. Proc. Natl. Acad. Sci. USA **70**: 3130–3133. doi:10.1073/pnas.70.11.3130

Litchman, E., P. de Tezanos Pinto, K. F. Edwards, C. A. Klausmeier, C. T. Kremer, and M. K. Thomas. 2015. Global biogeochemical impacts of phytoplankton: A trait-based perspective. J. Ecol. **103**: 1384–1396. doi:10.1111/1365-2745.12438

Lürling, M., F. Eshetu, E. J. Faassen, S. Kosten, and V. L. M. Huszar. 2013. Comparison of cyanobacterial and green algal growth rates at different temperatures. Freshw. Biol. **58**: 552–559. doi:10.1111/j.1365-2427.2012.02866.x

McGill, B. J., B. J. Enquist, E. Weiher, and M. Westoby. 2006. Rebuilding community ecology from functional traits. Trends Ecol. Evol. **21**: 178–185. doi:10.1016/j.tree.2006.02.002

Meunier, C. L., M. Boersma, R. El-Sabaawi, H. M. Halvorson, E. M. Herstoff, D. B. Van de Waal, J. V. Richard, and E. Litchman. 2017. From elements to function: Toward unifying ecological stoichiometry and trait-based ecology. Front. Environ. Sci. **5**: 18. doi:10.3389/fenvs.2017.00018

Mitchell, M., B. Muftakhidinov, and T. Winchen. 1991. Engauge Digitizer 4.1. Available from http://markummitchell.github.io/engauge-digitizer. Last Accessed: engauge-digitizer-v12.2.1. https://doi.org/10.5281/zenodo.3941227

Myklestad, S. M. 1995. Release of extracellular products by phytoplankton with special emphasis on polysaccharides. Sci. Total Environ. **165**: 155–164. doi:10.1016/0048-9697(95)04549-G

Oksanen, J., and others. 2015. Vegan: Community ecology package. R Package Version 22-1.

Oliver, R. L., and G. G. Ganf. 2000. Freshwater blooms: Their Diversity in Time and Space, p. 149–194. *In* B. A. Whitton and M. Potts [eds.], The ecology of cyanobacteria. Springer, Dordrecht.

Otero, A., and M. Vincenzini. 2003. Extracellular polysaccharide synthesis by *Nostoc* strains as affected by N source and light intensity. J. Biotechnol. **102**: 143–152. doi:10.1016/S0168-1656(03)00022-1

Paerl, H. W. 1988. Nuisance phytoplankton blooms in coastal, estuarine, and inland waters. Limnol. Oceanogr. **33**: 823–843. doi:10.4319/lo.1988.33.4part2.0823

Paerl, H. W., and D. F. Millie. 1996. Physiological ecology of toxic cyanobacteria. Phycologia **35**: 160–167. doi:10.2216/i0031-8884-35-6S-160.1

Paerl, H. W., and J. L. Pinckney. 1996. A mini-review of microbial consortia: Their roles in aquatic production and biogeochemical cycling. Microb. Ecol. **31**: 225–247. doi:10.1007/BF00171569

Paerl, H. W., and J. Huisman. 2009. Climate change: A catalyst for global expansion of harmful cyanobacterial blooms. Environ. Microbiol. Rep. **1**: 27–37. doi:10.1111/j.1758-2229.2008.00004.x

Peñuelas, J., and others. 2019. The bioelements, the elementome, and the biogeochemical niche. Ecology **100**: e02652. doi:10.1002/ecy.2652

Pereira, S., A. Zille, E. Micheletti, P. Moradas-Ferreira, R. De Philippis, and P. Tamagnini. 2009. Complexity of cyanobacterial exopolysaccharides: Composition, structures, inducing factors and putative genes involved in their biosynthesis and assembly. FEMS Microbiol. Rev. **33**: 917–941. doi:10.1111/j.1574-6976.2009.00183.x

Pfeifer, F. 2012. Distribution, formation and regulation of gas vesicles. Nat. Rev. Microbiol. **10**: 705–715. doi:10.1038/nrmicro2834

Qian, X., M. K. Kim, G. K. Kumaraswamy, A. Agarwal, D. S. Lun, and G. C. Dismuke. 2017. Flux balance analysis of photoautotrophic metabolism: Uncovering new biological details of subsystems involved in cyanobacterial photosynthesis. Biochim. Biophys. Acta Bioenerg. **1858**: 276–287. doi:10.1016/j.bbabio.2016.12.007

R Core Team, 2018. R: A language and environment for statistical computing. R Foundation for Statistical Computing, Vienna. https://www.R-project.org

Reynolds, C. S. 2006. The ecology of phytoplankton. Cambridge University Press.

Rodriguez-Molares, A., S. Dickson, P. Hobson, C. Howard, A. Zander, and M. Burch. 2014. Quantification of the ultrasound induced sedimentation of *Microcystis aeruginosa*. Ultrason. Sonochem. **21**: 1299–1304. doi:10.1016/j.ultsonch.2014.01.027

Sandrini, G., H. C. P. Matthijs, J. M. H. Verspagen, G. Muyzer, and J. Huisman. 2014. Genetic diversity of inorganic carbon uptake systems causes variation in CO_2 response of the cyanobacterium *Microcystis*. ISME J. **8**: 589–600. doi:10.1038/ismej.2013.179

Scott, J. T., M. J. McCarthy, and H. W. Paerl. 2019. Nitrogen transformations differentially affect nutrient-limited primary production in lakes of varying trophic state. Limnol. Oceanogr.: Lett. **4**: 96–104. doi:10.1002/lol2.10109

Smith, V. H. 2003. Eutrophication of freshwater and coastal marine ecosystems a global problem. Environ. Sci. Pollut. Res. **10**: 126–139. doi:10.1065/espr2002.12.142

Sterner, R. W., and J. J. Elser. 2002. Ecological stoichiometry: The biology of elements from molecules to the biosphere. Princeton University Press.

Stomp, M., J. Huisman, L. Vörös, F. R. Pick, M. Laamanen, T. Haverkamp, and L. J. Stal. 2007. Colourful coexistence of red and green picocyanobacteria in lakes and seas. Ecol. Lett. **10**: 290–298. doi:10.1111/j.1461-0248.2007.01026.x

Urbani, R., E. Magaletti, P. Sist, and A. M. Cicero. 2005. Extracellular carbohydrates released by the marine diatoms *Cylindrotheca closterium*, *Thalassiosira pseudonana* and *Skeletonema costatum*: Effect of P-depletion and growth status. Sci. Total Environ. **353**: 300–306. doi:10.1016/j.scitotenv.2005.09.026

Van de Waal, D. B., J. M. H. Verspagen, M. Lürling, E. van Donk, P. M. Visser, and J. Huisman. 2009. The ecological stoichiometry of toxins produced by harmful cyanobacteria: An experimental test of the carbon-nutrient balance hypothesis. Ecol. Lett. **12**: 1326–1335. doi:10.1111/j.1461-0248.2009.01383.x

Van de Waal, D. B., G. Ferreruela, L. Tonk, E. Van Donk, J. Huisman, P. M. Visser, and H. C. P. Matthijs. 2010. Pulsed nitrogen supply induces dynamic changes in the amino acid composition and microcystin production of the harmful cyanobacterium *Planktothrix agardhii*. FEMS Microbiol. Ecol. **74**: 430–438. doi:10.1111/j.1574-6941.2010.00958.x

Van de Waal, D. B., V. H. Smith, S. A. Declerck, E. C. Stam, and J. J. Elser. 2014. Stoichiometric regulation of phytoplankton toxins. Ecol. Lett. **17**: 736–742. doi:10.1111/ele.12280

Wagner, H., T. Jakob, A. Fanesi, and C. Wilhelm. 2017. Towards an understanding of the molecular regulation of carbon allocation in diatoms: The interaction of energy and carbon allocation. Philos. Trans. R. Soc. Lond. B Biol. Sci. **372**: 20160410. doi:10.1098/rstb.2016.0410

Wagner, N. D., F. S. Osburn, J. Wang, R. B. Taylor, A. R. Boedecker, C. K. Chambliss, B. W. Brooks, and J. T. Scott. 2019. Biological stoichiometry regulates toxin production in *Microcystis aeruginosa* (UTEX 2385). Toxins **11**: 601. doi:10.3390/toxins11100601

Walsby, A. E. 1994. Gas vesicles. Microbiol. Rev. **58**: 94–144.

Walsby, A. E., P. K. Hayes, R. Boje, and L. J. Stal. 1997. The selective advantage of buoyancy provided by gas vesicles for planktonic cyanobacteria in the Baltic Sea. New Phytol. **136**: 407–417. doi:10.1046/j.1469-8137.1997.00754.x

Wang, S., J. Xiao, L. Wan, Z. Zhou, Z. Wang, C. Song, Y. Zhou, and X. Cao. 2018. Mutual dependence of nitrogen and phosphorus as key nutrient elements: One facilitates *Dolichospermum flos-aquae* to overcome the limitations of the other. Environ. Sci. Technol. **52**: 5653–5661. doi:10.1021/acs.est.7b04992

Weithoff, G., and B. E. Beisner. 2019. Measures and approaches in trait-based phytoplankton community ecology – from freshwater to marine ecosystems. Front. Mar. Sci. **6**: 40. doi:10.3389/fmars.2019.00040

Wells, M. L., and others. 2015. Harmful algal blooms and climate change: Learning from the past and present to forecast the future. Harmful Algae **49**: 68–93. doi:10.1016/j.hal.2015.07.009

Wu, Z. X., and L. R. Song. 2008. Physiological comparison between colonial and unicellular forms of *Microcystis aeruginosa* Kütz (Cyanobacteria). Phycologia **47**: 98–104. doi:10.2216/07-36.1

Xu, H., H. W. Paerl, B. Qin, G. Zhu, and G. Gaoa. 2010. Nitrogen and phosphorus inputs control phytoplankton growth in eutrophic Lake Taihu, China. Limnol. Oceanogr. **55**: 420–432. doi:10.4319/lo.2010.55.1.0420

Zhao, H., W. Zhu, H. Chen, X. Zhou, R. Wang, and M. Li. 2017. Numerical simulation of the vertical migration of *Microcystis* (cyanobacteria) colonies based on turbulence drag. J. Limnol. **76**: 190–198. doi:10.4081/jlimnol.2016.1501

Zhu, G., and others. 2018*a*. Variation and driving factors of nutrients and chlorophyll-*a* concentrations in northern region of Lake Taihu, China, 2005–2017. J. Lake Sci. **30**: 279–295. doi:10.18307/2018.0201

Zhu, W., X. Zhou, H. Chen, L. Gao, M. Xiao, and M. Li. 2016. High nutrient concentration and temperature alleviated formation of large colonies of *Microcystis*: Evidence from field investigations and laboratory experiments. Water Res. **101**: 167–175. doi:10.1016/j.watres.2016.05.080

Zhu, W., Y. Tan, R. Wang, G. Feng, H. Chen, Y. Liu, and M. Li. 2018*b*. The trend of water quality variation and analysis in typical area of Lake Taihu, 2010-2017. J. Lake Sci. **30**: 296–305. doi:10.18307/2018.0202

Acknowledgments

This research was funded by the National Natural Science Foundation of China (32071569; awarded to XT), the China Postdoctoral Science Foundation (2020M681472; awarded to ZD), the Fundamental Research Funds for the Central Universities (B210202010; awarded to ZD), the China Scholarship Council (201806710165; awarded to ZD), the USA National Science Foundation (1831096 and 1840715; awarded to HWP), the KNAW Visiting Professors Programme (KNAW WF/RB/3781; awarded to HWP), and the Science and Technology Project of Jiangsu Province (BE2018737; awarded to XT). The authors thank Nico Helmsing and Dennis Waasdorp for assistance with the experimental setup, Nico Helmsing for elemental analyses, Erik Reichman and Iris Chardon for help with the chemical analyses, and Suzanne Wiezer for flow cytometer analyses. The authors also thank Petra Visser and Jolanda Verspagen from the University of Amsterdam for the possibility to use their setup to measure gas vesicles, and Guangwei Zhu and Nanjing Institute of Geography and Limnology, Chinese Academy of Sciences (NIGLAS) for providing permission redrawn for Fig. 6a.

Conflict of Interest

None declared.

Submitted 13 November 2020
Revised 06 February 2021
Accepted 11 March 2021

Associate editor: Michele Burford